Journal of Microwaves, Optoelectronics and Electromagnetic Applications, Vol. 21, No. 1, March 2022
DOI: http://dx.doi.org/10.1590/2179-10742022v21i11380

MIMO-PLC Communications in an Experimental Medium Voltage Network: Measurement and Analysis

Ulysses R. C. Vitor[1], Matheus Cabral [1], Daniel Fonseca[1], Lauro R. G. S. L. Novo[2], Marcos T. de Melo[2], Marcelo E. V. Segatto[3], Gabriel G. Machado[4]

[1]*Universidade Federal de Juiz de Fora, Juiz de Fora, Minas Gerais, Brasil, ulysses.vitor@engenharia.ufjf.br, matheus.cabral@engenharia.ufjf.br, daniel.fonseca@engenharia.ufjf.br*

[2]*Universidade Federal de Pernambuco, Recife, Pernambuco, Brasil, lauro.no@ufpe.br, marcostdemelo@gmail.com*

[3]*Universidade Federal do Espirito Santo, Vitoria, Espirito Santo, Brasil, marcelo.segatto@gmail.com*

[4]*The Institute of Electronics, Communications and Information Technology (ECIT), Queen's University of Belfast, Belfast, United Kingdom, g.machado@qub.ac.uk*

***Abstract*– This paper presents measurements at a mock-up medium voltage network to verify the feasibility of Broadband Power Line Communication (BPLC). We use the data extracted within the frequency range $2-30$ MHz to characterize a MIMO PLC network using different phase combinations, defining the best and worst use case scenarios. The empirical data shows that not only phases directly connected for input-output can be used, but also that we can exploit the coupling between phases to transmit and receive data, therefore creating a dynamic PLC network which will depend on the characteristics of the power grid. By making use of transmission line theory, we also demonstrate how we can mitigate the reflections by measuring the input impedance of the network to allow better use of the bandwidth available for BPLC operation.**

***Index Terms*–** MIMO, BPLC, Input Impedance, Broadband, Medium voltage.

I. Introduction

The Information Age, with its start in the mid-20$^{\text{th}}$ century, has witnessed a fast advancement in communications systems in recent years, enabling interconnected technologies such as the Internet of Things (IoT). The need to always achieve higher data transmission rates has attracted investment from large companies into research institutes and universities. Therefore, devising new means to reduce costs to increase the communication system capacity naturally comes up as a priority to the industry. Wireless communications proved to be a great solution to overcome this issue, however covering large areas is still a topic of scientific interest from which challenges still needs to be addressed [1]. In this manner, Power Line Communication (PLC) technology seeks to bring an efficient and cheaper way of communication for several applications, such as in regions where access is more difficult due to the distance or the geography of the place [2], [3].

This technology is divided into two categories: narrow band (NPLC) and broadband (BPLC). The former is often used for remote control and measurement of energy, gas and water [4] in the frequency range from 9 kHz to 140 kHz. The latter works in frequencies up to 100 MHz and is used to transmit voice, video and data at high rates [2], [3], [5], [6].

A challenge faced by PLC technology is its own hostile environment as the electrical network

Brazilian Microwave and Optoelectronics Society-SBMO *received 1 June 2021; for review 10 June 2021; accepted 7 Dec 2021*
Brazilian Society of Electromagnetism-SBMag *ISSN 2179-1074*

presents problems for data transmission. For example, noise, multi-path, impedance mismatch and frequency selectivity are factors that need to be considered when designing a PLC communication system. To overcome such problems, Orthogonal Frequency-Division Multiplexing (OFDM) modulation was adopted, which uses several orthogonal subcarriers. This type of modulation offers great adaptability to the system as it is capable to suppress interfering or interfered carriers and vary the load (number of bits) of each carrier according to the signal to noise ratio (SNR) or link attenuation [2], [3].

Advanced signal processing techniques allowed data transmission in broadband PLC more efficiently. Nowadays, there are devices on the market that can reach up to 205 Mbps [7]. Such equipment was used in a medium voltage grid to monitor oil platforms and excellent performance has been reported [8], [9].

Such devices have several modes of operation within different bandwidths (5, 10 or 30 MHz), transmission rate and Power Spectral Density (PSD) [7]. These operation modes associated with MIMO techniques, such as space–time parallel intercarrier interference (ICI) cancellation of OFDM [10], provides an efficient use of the Medium Voltage Grid to transmit data. In addition, modern gateways such as [7] are able to transmit with a power spectrum density (PSD) of -50 dBm/Hz whilst receivers could operate up to -72 and -77 dBm/Hz [7], with the reported capability of working within the threshold of -22 dB/Hz of attenuation.

PLC channel modelling has been investigated by several groups in the open literature such as [11]–[14]. In [11], the authors demonstrated that caching popular content into each PLC access unit, and designing a precoding scheme using MIMO techniques on the PLC channel can improve the data transmission and offer a better price model for the end-users. In [12], the influence of dielectric in a three-core power cable is evaluated, where the phase-mode transformation is used to decompose the per-unit-length parameters into common-mode and differential-mode parameters, combining numerical and measured data to build a robust model for MIMO PLC channel modeling. In [13], the authors investigated a mixed channel comprised of a medium voltage network, underground and overhead [13]. Finally, digital simulations were carried out in a medium voltage MIMO PLC network in [14], to evaluate the performance using MIMO-OFDM techniques, where the authors designed an encoder and optimized key decoder parameters to reduce the bit error rate, demonstrating that medium voltage MIMO-OFDM is a good approach to provide high data rate and link reliability to PLC channels.

In our literature review, to the best of our efforts, no other work which performs the characterization of the frequency response and impedance of the MIMO-PLC network was found. Our work brings two contributions to this field, first we report that the most of the BPLC frequency range is suitable to transmit data. This is achieved by carrying out measurements in a mock-up three phases medium voltage grid. The phase combination features a channel with nine paths or three possible inputs and three outputs. The second comes as an estimation of the network input impedance to design more efficient medium voltage couplers, with this information it is possible to use an adaptive coupler [15] more efficiently.

The organization of this work is as follows. In Section II we present the concept of transmission lines and PLC channel, delivering a theoretical support to this article. Also in this section, the topology for the investigated scenarios are presented. Section III discusses the experimental setup, the instruments and equipment used. In Section IV, the results for the experiments performed in the mock-up transmission line are analyzed . Finally, Section V presents the conclusions and the potential of this research for

Brazilian Microwave and Optoelectronics Society-SBMO *received 1 June 2021; for review 10 June 2021; accepted 7 Dec 2021*
Brazilian Society of Electromagnetism-SBMag *ISSN 2179-1074*

further studies.

II. Theoretical Analysis

Figure 1 depicts an N ports network, the scattering parameters (S-Parameters) relate the incident and reflective voltage waves for each port which we consider to be the inputs and outputs of the PLC grid [16]. The relation between V_i^- and V_i^+ is shown in (1) and (2).

$$\begin{bmatrix} V_1^- \\ V_2^- \\ \vdots \\ V_N^- \end{bmatrix} = \begin{bmatrix} S_{11} & S_{12} & \cdots & S_{1N} \\ S_{21} & & & \\ \vdots & & \ddots & \vdots \\ S_{N1} & & & S_{NN} \end{bmatrix} \begin{bmatrix} V_1^+ \\ V_2^+ \\ \vdots \\ V_N^+ \end{bmatrix} \tag{1}$$

where

$$S_{ij} = \left. \frac{V_i^-}{V_j^+} \right|_{V_k^+ = 0 \; for \; k \neq 0} \tag{2}$$

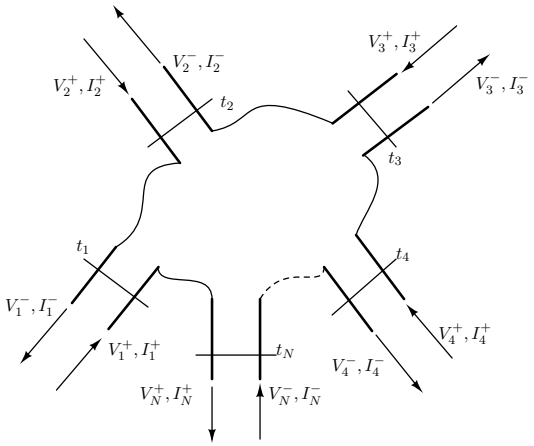

Fig. 1. Representation of a N ports networks.

Broadband PLC signal travel through Transverse Electromagnetic (TEM) mode on electric distribution line which allows the application of traditional transmission line (TL) theory, well known and published in the open literature [3], [5], [17], [18]. The analysis method of a TL is facilitated by modeling electrical circuits, consisting of resistances per unit length, R (Ω/m), capacitance per unit length, C (F/m), inductance per unit length, L (H/m), and conductance per unit length, G(1/Ωm) [16], [18], [19].

Considering the three phases and the propagation in the z direction, one can derive the model of an infinitesimal (Δz) part of the line, as shown in Fig. 2. Additionally, the equivalent transmission line for phases A and B is provided in Fig. 3, where R_{eq}, L_{eq}, G_{eq} and C_{eq} are the equivalent resistance, inductance, conductance and capacitance from Fig. 2.

Knowing that the input impedance of a data receiver is 50 Ω, the input impedance for this line is given by (3) [16], [20]. Therefore, one can calculate the TL input impedance and thus design PLC couplers for injection and reception of the network signal [21].

Brazilian Microwave and Optoelectronics Society-SBMO *received 1 June 2021; for review 10 June 2021; accepted 7 Dec 2021*
Brazilian Society of Electromagnetism-SBMag *ISSN 2179-1074*

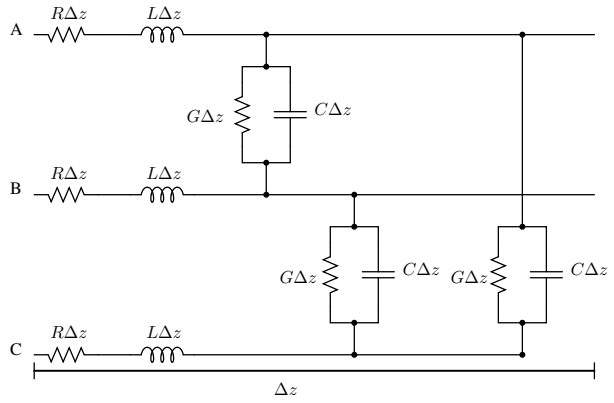

Fig. 2. Model of circuits for three-phase.

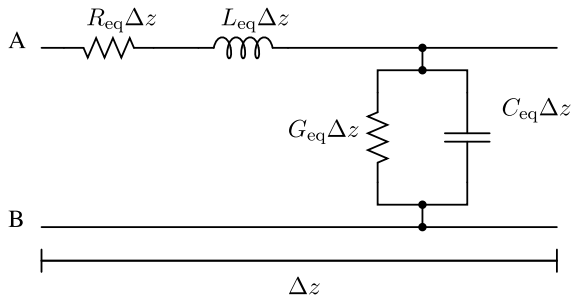

Fig. 3. Equivalent lumped-element circuit of two wires transmission line.

$$Z_{in} = 50\left[\frac{1+S_{11}}{1-S_{11}}\right] \tag{3}$$

Assuming the three-phase system, phases A, B and C, when a signal is injected in the MHz range in phase A, it induces a current in phases B and C, similar to an antenna behaviour. This is true for all three phases in the system and therefore needs to be considered in the modelling of the TL [3], [17].

Moreover, the medium voltage PLC network investigated in our study can be analyzed as a six ports network, where three are input ports and the remainder are output ports. The ports are combinations of phases two by two. Thus, in both input and reception there are 3 signal injection possibilities (three combinations of two). This representation is depicted in Fig. 4.

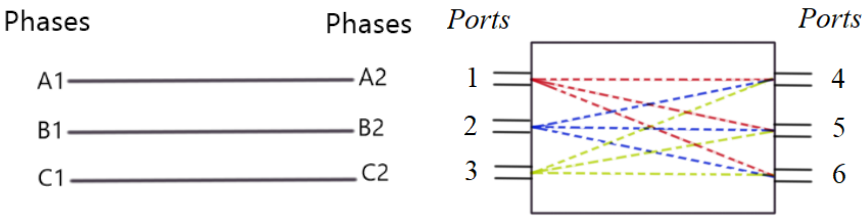

Fig. 4. MIMO model corresponding to the three-phase system [22].

In the general case of a MIMO system comprising of three emitter ports and three receiver ports, the channel matrix H can be written as [22], [23]:

ISSN 2179-1074

$$H = \begin{bmatrix} h_{11} & h_{12} & h_{13} \\ h_{21} & h_{22} & h_{23} \\ h_{31} & h_{32} & h_{33} \end{bmatrix} \tag{4}$$

According to Fig. 4, there are 9 possible topologies, considering the point of injection of the signal, represented by A1, B1 and C1, and at the other end represented by A2, B2 and C2.

The Vector Network Analyzer (VNA) measurements are named X1Y1 for the input port from signals applied in the phases X and Y, and likewise X2Y2 for the output port from signals measured from the X and Y, where X and Y could be A, B or C. As shown in Table I, it is possible to see all port representation measurements related to cases from 1 to 9 given by the previous two-by-two combinations:

TABLE I. POSSIBLE COMBINATIONS FOR THE SYSTEM PORTS

Topology	**Input Port**	**Output Port**
Case 1	A1B1	A2B2
Case 2	A1B1	A2C2
Case 3	A1B1	B2C2
Case 4	A1C1	A2B2
Case 5	A1C1	A2C2
Case 6	A1C1	B2C2
Case 7	B1C1	A2B2
Case 8	B1C1	B2C2
Case 9	B1C1	C2A2

To analyze the system using S-Parameters, based on (4), the channel matrix can be obtained from the VNA measurements, which is represented in (5), where C_i refers to Case *i*, with *i* ranging from 1 to 9, see Table I.

$$H = \begin{bmatrix} S_{21}^{C_1} & S_{21}^{C_2} & S_{21}^{C_3} \\ S_{21}^{C_4} & S_{21}^{C_5} & S_{21}^{C_6} \\ S_{21}^{C_7} & S_{21}^{C_8} & S_{21}^{C_9} \end{bmatrix} \tag{5}$$

III. EXPERIMENTAL SETUP

The experimental set-up is shown in Fig. 5, where the network structure comprised of 8, 2 meters tall, utility poles spaced 5 meters apart, and a U-shaped turn from pole 5 to 6 (starting from phases A1, B1 and C1) is depicted. In this work, the experiments were carried out connecting the VNA - R&S®Network Analyzer 9 kHz - 6 GHz and two extended 50 Ω-coaxial cables in the available three-phase distribution line, whilst those were disconnected from the live power grid during the experiment. Each phase of the medium voltage network is made of a 3/8 inch aluminium cable and located 2.3 meters above the ground.

received 1 June 2021; for review 10 June 2021; accepted 7 Dec 2021

ISSN 2179-1074

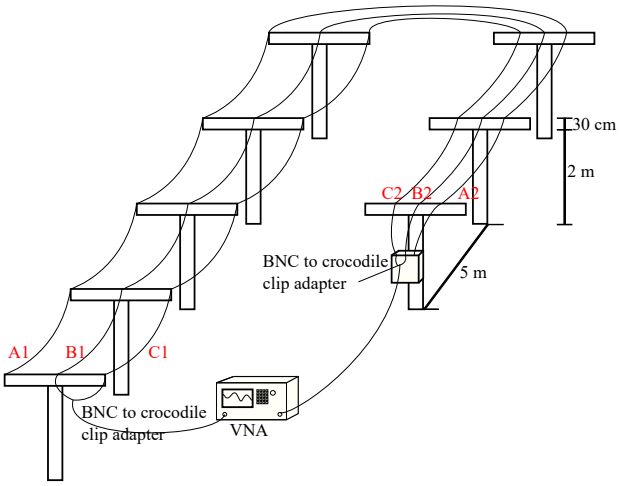

Fig. 5. Experimental set-up in the mock-up three-phase distribution line.

The example shown in Fig. 5 represents the experimental arrangement equivalent to Case 8, i.e., S_{21} and S_{11} measurements were carried out, where B1C1 and B2C2 are the input and output ports, respectively. Two coaxial cables were connected to both ports of the VNA through BNC (Bayonet Neill Concelman) connectors, where Port 1 was connected as transmitter and Port 2 as receiver, therefore obeying the system proposed in (5). For Case 8, as depicted in Fig. 5, the signal is injected into phases B1 and C1 of the power grid via BNC to crocodile clip adapters, whilst the signal is received at phases B2 and C2. Due to its symmetry it is only necessary to measure in one direction [16].

Once the test network is not energized (live), medium voltage couplers were not necessary. For this reason, and due to lack of available resources to properly calibrate the VNA to this unique set-up, the measurements were not calibrated. As a result, we expected more reflections than in a real scenario where couplers are used which will provide a wider bandwidth to data transmission. Additionally, we expected an attenuation of ≈ 0.1 dB/m due to the alligator clips with coaxial cable for frequencies up to 30 MHz [24]. Finally, the resistivity of aluminium at 20°C is 28.2 $n\Omega$m [25], whereas during our measurements at 12 noon with a temperature of $\approx$ 30°C, this can increase to 29.4 $n\Omega$m, which for a 35 m line represents a variation of $\approx 4.3\%$ in the total resistance of the line, when linear thermal expansion approximation is used as shown in (6) [26], where $\alpha_{\mathrm{Al}} = 0.00429°\mathrm{C}^{-1}$ is the temperature coefficient of resistivity of aluminum. However, for small fluctuations of up to 2°C at 30°C, the variation is of just 0.85%, and therefore were not accounted for in our results.

$$\rho = \rho_0[1 + \alpha_{\mathrm{Al}}(T - T0)] \tag{6}$$

The phases which were not associated with the measurement being performed (for a specific case), were left open. Thus, it can be said that the signal reflected from the open phases is negligible due to the high attenuation of the network and the distance between the ports. So the scattering matrix parameters can be considered equal to the coefficient of reflection and transmission of the network.

IV. Results and Analysis

For our reference, the previously mentioned device from Corinex technology [7], reports good performance on channels with attenuation of up to 22 dB. Here, we use this value to define the

ISSN 2179-1074

useful bandwidth for data transmission, where the S_{21} is higher than -20 dB as we assume a total 2 dB attenuation in the coaxial cables + crocodile clips.

First, we will analyze the cases in which VNA ports 1 and 2 are connected to their matching phases, i.e., the direct paths for transmission of information. These are cases 1, 5 and 8 previously described in Table I, and plotted in Fig. 6, which shows the measured insertion loss in dB, whilst the red line marks the -20 dB threshold discussed previously. From these results, we observe that a good portion of the bandwidth can potentially be used for the transmission of PLC signal, which indicates that one can choose the configuration that will provide the best transmission characteristics depending on the band available on a certain scenario. For example, Case 1 shows that the frequency range $10.5-15.1$ MHz is suitable for the application of the signal, whilst the region between $10.5-21.2$ MHz is 100% available in Case 8, where the extra bandwidth might be useful for applications requiring higher data-rates.

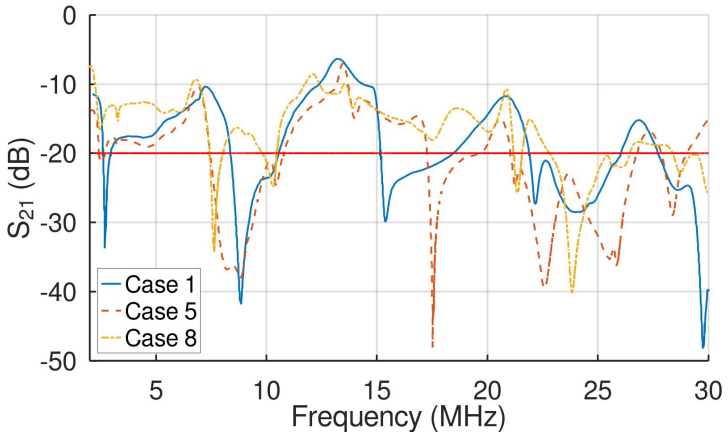

Fig. 6. Measured results of the S_{21} magnitude for cases 1, 5 and 8, with the red line highlighting the -20 dB thershold.

Moreover, we investigated the cases where the coupling between lines takes effect. For cases 2 and 3, the one of the input phases is different from the output, see Table I. As a result, a greater frequency selectivity is observed as shown in Fig. 7. In both cases high levels of attenuation are noticed at frequencies above 20 MHz, making this spectrum range unavailable. A similar scenario is observed in Fig. 8, which refers to cases 4 and 6, where most of the band up to 21.77 MHz is available for data transmission in Case 4 and 18.27 MHz for Case 6. For the latter, almost all the measured range between $2-18.27$ MHz can potentially be used for broadband data transmission using PLC signal.

Finally, Fig. 9 shows the possible frequency bands available for cases 7 and 9. In Case 7, almost all the band up to 21.6 MHz is available with a few transmission nulls. On the other hand, Case 9 does not present wide regions available for transmission where most of the band is available to frequencies up to ≈ 15 MHz.

received 1 June 2021; for review 10 June 2021; accepted 7 Dec 2021

ISSN 2179-1074

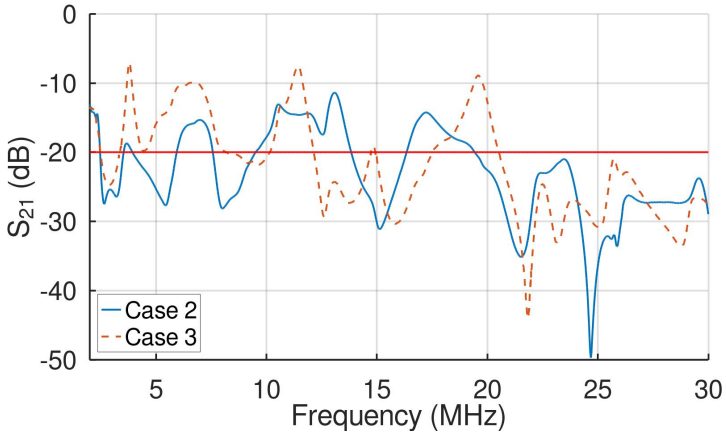

Fig. 7. Measured results of the S_{21} magnitude for cases 2 and 3.

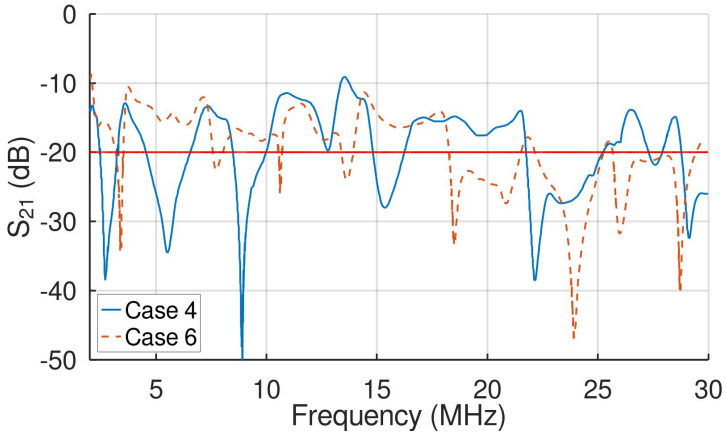

Fig. 8. Measured results of the S_{21} magnitude for cases 4 and 6.

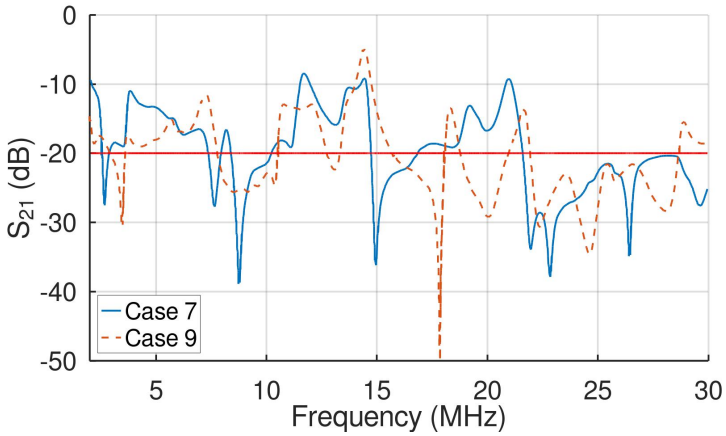

Fig. 9. Measured results of the S_{21} magnitude for cases 7 and 9.

To summarize the information, Table II shows the available bandwidth for the measured frequencies between $2 - 30$ MHz. Case 8, with a direct path between both phases has presented the best results in terms of bandwidth utilization, followed by cases 4 and 6. We notice that in these situations, phase B is always connected to port 2 of the VNA. The worst results are observed for cases 2 and 3, where phase C is connected to port 2.

TABLE II. BANDWIDTH FOR EACH CASE

Topology	**Δf (MHz)**	**Δf (%)**
Case 1	15.764	56.3
Case 2	9.884	35.3
Case 3	10.584	37.8
Case 4	16.968	60.6
Case 5	15.176	54.2
Case 6	16.408	58.6
Case 7	14.784	52.8
Case 8	21.252	75.9
Case 9	12.824	45.8

Furthermore, to perform the impedance matching between a PLC switch and the grid, the input impedance must be known. By solving the impedance mismatch issue, one can expect that the attenuation of the PLC signal will only caused by the ohmic losses of the channel.

In a real model, loads dynamically change across the network throughout the day. This leads to a change in the input impedance, and therefore in S_{11} and S_{21}. Therefore, for each case depicted in Table II, variations in bandwidth are expected. As a consequence of these variations, the PLC modem will dynamically change the data allocation in the OFDM channels [7] to maintain high transmission rates.

As previously shown in (3), the input impedance of the network can be calculated when S_{11} is known. Afterwards, it is possible to dynamically switch the output and input impedance of the transmitter for different frequency bands to optimize matching and reduce reflections.

Figure 10 depicts the module and phase of the input impedance for cases 7 and 8. It is noticed that impedance mismatch occurs for the most part of the spectrum, whilst $Z_{in} < 300\ \Omega$. The plots are of a similar behavior, except at 7 MHz where a difference of 100 Ω in the input impedance is observed.

For cases 2, 3, 6 and 9, we observe peaks for $|Z_{in}|$, reaching values between 500 Ω and 600 Ω, as depicted in Fig. 11. When compared to Z_{in} in Fig. 10, the shapes show a certain similarity, despite the higher peaks observed in the latter. We also observe that cases 2 and 3 are very similar, which also occurs between cases 6 and 9. However, these two sets differ by a shift in the impedance module and phase.

For the remaining cases, we notice a peak greater than 600 Ω. In addition, peaks at frequencies greater than 20 MHz have been reduced as shown in Fig. 12.

In a scenario where an adaptive coupler which is capable of delivering a variable output impedance, we would be able to reduce the signal reflection for each frequency band. These impedance plots show that our mock-up medium voltage power grid has a higher potential to transmit MIMO PLC signal than the results previously presented from Fig. 6 to 9. Therefore, higher data transmission rates can be achieved by dynamically allocating the frequency bands dedicated to the PLC channel.

Brazilian Microwave and Optoelectronics Society-SBMO *received 1 June 2021; for review 10 June 2021; accepted 7 Dec 2021*
Brazilian Society of Electromagnetism-SBMag *ISSN 2179-1074*

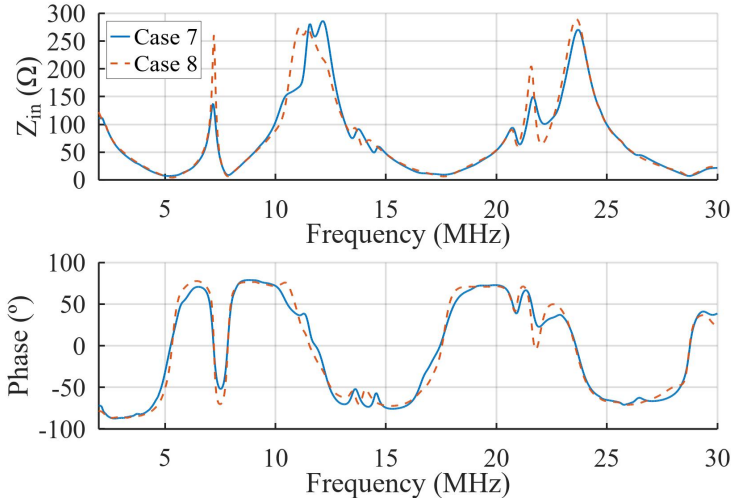

Fig. 10. Computed results of the Z_{in} magnitude and phase for cases 7 and 8.

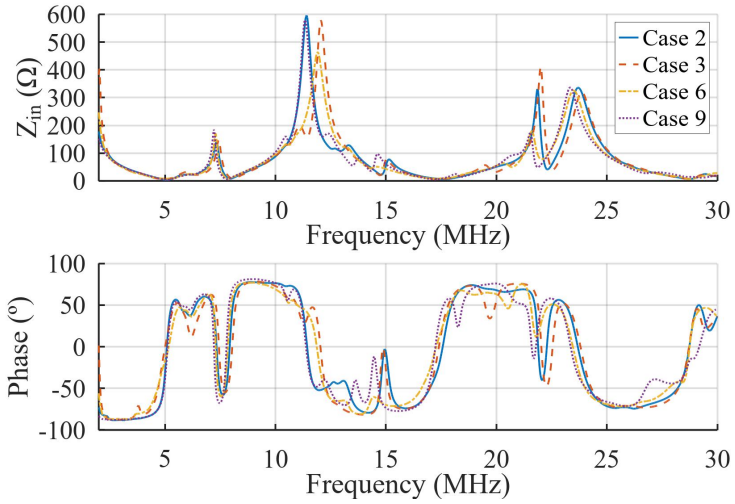

Fig. 11. Computed results of the Z_{in} magnitude and phase for cases 2, 3, 6 and 9.

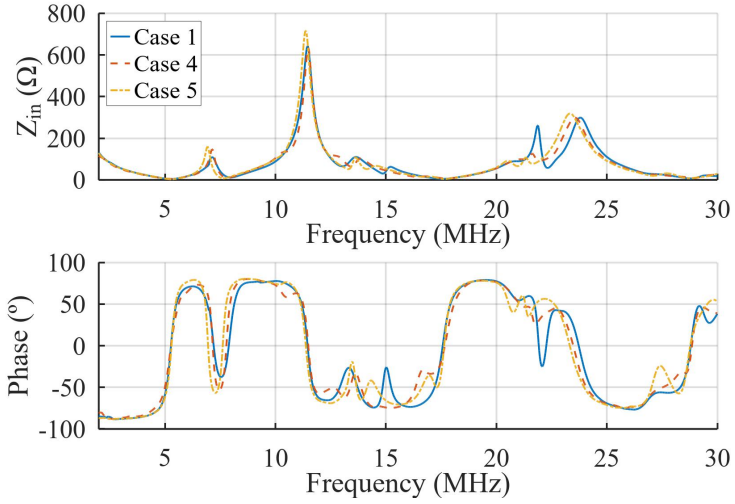

Fig. 12. Computed results of the Z_{in} magnitude and phase for cases 1, 4 and 5.

Brazilian Microwave and Optoelectronics Society-SBMO *received 1 June 2021; for review 10 June 2021; accepted 7 Dec 2021*
Brazilian Society of Electromagnetism-SBMag

ISSN 2179-1074

V. CONCLUSIONS

In this paper, we proposed a new technique for characterizing a PLC channel using the S-Parameters to obtain the H matrix of a mock-up medium voltage electrical network. Our empirical data showed that it is feasible to make use of the network under test for broadband PLC, even in hostile environments for data transmission. Furthermore, it is possible to employ MIMO techniques to obtain a better performance than when the signal is injected into one phase or splitting it into two phases as usually found in BPLC applications. Finally, we show that by extracting the input impedance of the network, it is possible to design couplers that are optimized to reduce reflections caused by impedance mismatch and further increase the effective data transmission rate. As a result, this work demonstrate feasibility of using the electrical network for broadband data transmission. In addition, our methodology can potentially be used as a reference to characterize low, medium and high voltage networks and expand the scenarios and capabilities of BPLC technology.

ACKNOWLEDGMENTS

This study was financed in part by the Coordenação de Aperfeiçoamento de Pessoal de Nível Superior - Brasil (CAPES) Finance Code 001.

REFERENCES

[1] S. D. Assimonis, M. A. B. Abbasi, and V. F. Fusco, "Millimeter-wave multimode circular array for spatially encoded beamforming in a wide coverage area," in *2021 15th European Conference on Antennas and Propagation (EuCAP)*, pp. 1–4, 2021.

[2] K. Dostert, *Powerline Communication*. Prentice Hall, 2001.

[3] R. L. Halid Hrasnica, Abdelfatteh Haidine, *Broadband Powerline Communication*. John Wiley & Sons, 2004.

[4] N. Shlezinger and R. Dabora, "On the capacity of narrowband plc channels," *IEEE Transactions on Communications*, vol. 63, no. 4, pp. 1191–1201, 2015.

[5] U. R. C. Vitor and M. T. de Melo, "Comparison between power line communication multipath model and coaxial cable interferometer theory," *International Journal of Communication Systems*, vol. 27, no. 1, pp. 151–162, 2012. [Online]. Available: https://onlinelibrary.wiley.com/doi/abs/10.1002/dac.2353

[6] "Ieee standard for broadband over power line networks: Medium access control and physical layer specifications," *IEEE Std 1901-2020 (Revision of IEEE Std 1901-2010)*, pp. 1–1622, 2021.

[7] "Manual técnico do modem cxp-hda-gwyc," in *User Guide*, 2014. [Online]. Available: https://svn.wirelessleiden.nl/svn/projects/nodebouwdocumentatie/Corinex_CXP-HDC_LVC_UserGuide_v1.0.pdf

[8] L. R. M. Castor, R. Natale, J. A. P. Favero, J. A. L. Silva, and M. E. V. Segatto, "The Smart Grid Concept in Oil & Gas Industries by a Field Trial of Data Communication in MV Power Lines," *Journal of Microwaves, Optoelectronics and Electromagnetic Applications*, vol. 15, pp. 81 – 92, 06 2016. [Online]. Available: http://www.scielo.br/scielo.php?script=sci_arttext&pid=S2179-10742016000200081&nrm=iso

[9] L. R. M. Castor, "A rede de média tensão como meio de transporte de dados em redes smart grid," in *Dissertação apresentada ao Programa de Pós-Graduação em Engenharia Elétrica do Centro Tecnológico da Universidade Federal do Espírito Santo, como requisito parcial para obtenção do Grau de Mestre em Engenharia Elétrica.*, 2015. [Online]. Available: https://repositorio.ufes.br/bitstream/10/9652/1/tese_7535_Leonardo%20Ribas%20Martins%20Castor.pdf

[10] A. Fadaei Tehrani, H.-G. Yeh, and S.-C. Kwon, "Ber performance of space–time parallel ici cancellation of ofdm in mimo power line communications," *IEEE Systems Journal*, vol. 15, no. 2, pp. 1742–1752, 2021.

[11] Y. Qian, S. Li, L. Shi, J. Li, F. Shu, D. N. K. Jayakody, and J. Yuan, "Cache-enabled mimo power line communications with precoding design in smart grid," *IEEE Transactions on Green Communications and Networking*, vol. 4, no. 1, pp. 315–325, 2020.

[12] Y. Guo, Z. Yang, R. Huo, and Z. Xie, "Channel model for low voltage three-core power line communication," *IEEE Access*, vol. 7, pp. 154 882–154 888, 2019.

received 1 June 2021; for review 10 June 2021; accepted 7 Dec 2021

ISSN 2179-1074

[13] Y. Lu, C. An, H. Gao, and J. Ye, "Channel characteristics analysis of medium voltage overhead and mixed overhead/underground cable power network," in *2020 IEEE 20th International Conference on Communication Technology (ICCT)*, pp. 44–50, 2020.

[14] Y. Li, M. Zhang, W. Zhu, M. Cheng, C. Zhou, and Y. Wu, "Performance evaluation for medium voltage mimo-ofdm power line communication system," *China Communications*, vol. 17, no. 1, pp. 151–162, 2020.

[15] L. G. Costa, A. Queiroz, V. Costa, and M. Ribeiro, *An Analog Filter Bank-based Circuit for Performing the Adaptive Impedance Matching in PLC Systems*, vol. 36, no. 1, pp. 133–150, Aug. 2021. [Online]. Available: https://jcis.sbrt.org.br/jcis/article/view/768

[16] D. M. Pozar, *Microwave Engineering*. John Wiley & Sons, 2011.

[17] U. R. C. Vitor, "Internet via rede elétrica: Modelagem de canal baseada em interferômetro," in *Dissertação submetida ao Programa de Pós-Graduação em Engenharia Elétrica da Universidade Federal de Pernambuco como Parte dos requisitos para obtenção do grau de Mestre em Engenharia Elétrica*, 2008.

[18] M. N. Sadiku, *Elementos de Eletromagnetismo*. Bookman, 2012.

[19] D. K. Cheng, *Fundamental of Engineering Electromagnetics*. Reading MA. Addison-Wesley, 1992.

[20] L. G. da S. Costa, G. R. Colen, A. C. M. de Queiroz, V. L. da Costa, U. R. C. Vitor, F. V. dos Santos, and M. V. Ribeiro, "Access impedance in brazilian in-home, broadband and low-voltage electric power grids," *Electric Power Systems Research*, vol. 171, pp. 141–149, 2019. [Online]. Available: https://www.sciencedirect.com/science/article/pii/S037877961930080X

[21] G. Artale, A. Cataliotti, V. Cosentino, S. Guaiana, D. Di Cara, N. Panzavecchia, G. Tinè, and R. Fiorelli, "An innovative coupling solution for power line communication in mv electrical networks," in *2019 1st Global Power, Energy and Communication Conference (GPECOM)*, pp. 90–95, 2019.

[22] P. P. Lars Torsten Berger, Andreas Schwager and D. Schneider, *MIMO Power Line Communications: Narrow and Broadband Standards, EMC, and Advanced Processing*. CRC Press, 2017.

[23] W. Z. Y. Li, M. Zhang, C. Z. M. Cheng, and Y. Wu, "Performance evaluation for medium voltage mimo-ofdm power line communication system," in *in China Communications*, vol. 17, no. 1, pp. 151–162, Jan. 2020.

[24] P. Minipa, "Ponta de prova mtl-21 - minipa," in *Bau Eletrônica*, 2021. [Online]. Available: https://www.baudaeletronica.com.br/ponta-de-prova-mtl-21-minipa.html

[25] A. Marie Helmensine, "A Table of Electrical Conductivity and Resistivity of Common Materials." [Online]. Available: https://www.thoughtco.com/table-of-electrical-resistivity-conductivity-608499

[26] R. R. David Halliday and J. Walker, *Fundamentos de Física - Eletromagnetismo*. LTC, 2003, vol. 3.

received 1 June 2021; for review 10 June 2021; accepted 7 Dec 2021

ISSN 2179-1074